ChemPubSoc Europe

DOI: 10.1002/cctc.201300356

A First-Principles DFT Study on the Active Sites of Pd-Cu-Cl_x/Al_2O_3 Catalyst for Low-Temperature CO Oxidation

Changli Shen,[a] Huiying Li,[a] Jun Yu,[a] Guisheng Wu,[a] Dongsen Mao,[a] and Guanzhong Lu*[a, b]

Research on the CO low-temperature oxidation has been a hot and important topic with regard to commercial applications and academic interest. Commercially, it can be widely used, for example, in indoor air cleaning, automotive exhaust treatment, CO_2 lasers, breathing apparatus, and fuel cells. In academia, findings and general laws established regarding CO oxidation will set solid foundations for the catalytic oxidation theory.

For the catalysts used in low-temperature CO oxidation, water resistance and catalyst stability are still serious challenges,[1,2] including for the recently studied catalyst Pd-Cu-Cl_x/γ-Al_2O_3.[3–5] It is generally believed that the overall catalytic chemistry of supported Wacker-type catalysts for CO oxidation is similar to that of the homogeneous Wacker catalyst (Pd-Cu-Cl_x), which is expressed in Equation (1):[6]

$$CO + PdCl_2 + H_2O \rightarrow CO_2 + Pd^0 + 2\,HCl \quad (1a)$$

$$Pd^0 + 2\,CuCl_2 \rightarrow PdCl_2 + 2\,CuCl \quad (1b)$$

$$2\,CuCl + 2\,HCl + 1/2\,O_2 \rightarrow 2\,CuCl_2 + H_2O \quad (1c)$$

The working mechanism of the Wacker catalyst suggested above shows that $PdCl_2$ is reduced to Pd^0 by CO, then Pd^0 is oxidized by $CuCl_2$, and finally CuCl is reoxidized by O_2. However, this mechanism has some unknown details to be explored, even resulting in some debates.[7] The nature of the Pd and Cu species is still unclear and a contentious issue. Kim and Lee et al.[8] reported that direct interaction of Pd–Pd or Pd–Cu was not detected and the Cl anion was transferred between Pd and Cu species in the redox process. Most researchers believed that the active Cu phase was hydroxylated CuCl rather than $CuCl_2$, CuCl, and CuO.[9–12] However, the Wacker catalyst would be deactivated quickly without water vapor, resulting in its color changing from green to gray. Hence, hydroxyl groups play an important role in the interaction (or the catalytic cycle) between Pd and Cu.[9] How oxygen is activated and how water promotes the oxidation reaction is still unclear.

[a] C. Shen,[+] Dr. H. Li,[+] J. Yu, Prof. G. Wu, Prof. D. Mao, Prof. G. Lu
Research Institute of Applied Catalysis
Shanghai Institute of Technology
100 Haiquan Road, Shanghai 201418 (P. R. China)
Fax: (+86) 21-60877231
E-mail: gzhlu@ecust.edu.cn

[b] Prof. G. Lu
Research Institute of Industrial catalysis
East China University of Science and Technology
130 Meilong Road, Shanghai 200237 (P. R. China)

[+] These authors contributed equally to this work.

Supporting information for this article is available on the WWW under http://dx.doi.org/10.1002/cctc.201300356.

A DFT calculation is a powerful tool for the catalysis study and probing reaction mechanisms. In the theoretical study on heterogeneous catalysis, researches have focused mainly on single metal or metal oxide catalysts.[13,14] For the catalysts with two kinds of active sites, such as supported Wacker catalysts (Pd-Cu-Cl_x), detailed studies on the catalytic reaction mechanism using simulation calculation have not been reported. Therefore, understanding the catalysis and active sites of supported Wacker catalyst is very important and significant for the design of an effective catalyst for CO oxidation and for enriching catalysis chemistry of multi-components catalysts with two kinds of active sites. Herein, the catalytic mechanism of the Wacker catalyst for CO oxidation was investigated by using DFT calculations and in situ diffuse-reflectance infrared Fourier transform spectroscopy (DRIFTS) characterization.

The Pd-Cu-Cl_x/Al_2O_3 catalyst was prepared by an NH_3 coordination–impregnation method.[3,12] All calculations were performed with the Perdew–Wang 91 functional by using the Vienna Ab initio Simulation Package (VASP)[15] and the calculation details described in the Experimental Section. The γ-Al_2O_3(100) crystal face model is shown in Figure S1; $PdCl_2$, PdCl, $CuCl_2$, and CuCl located on the γ-Al_2O_3 surface are shown in Figures S1 and S2, and their relative structural parameters are presented in Tables S1 and S2.

Firstly, CO adsorptions on $PdCl_2$, $CuCl_2$, PdCl, and CuCl in the absence of O_2 and H_2O were calculated by using DFT. The results show that CO cannot adsorb on $PdCl_2$ and $CuCl_2$ in the steady state, which is consistent with the anaylsis of the in situ DRIFTS spectra (Figure 1c). As seen in Figure 1c, the absorption peak of Pd^{2+}–CO at 2162 cm^{-1} is initially weak and disappears quickly with an increase in contact time and the absorption peak of Cu^{2+}–CO cannot be detected. DFT calculations show that the Pd^{2+} and Cu^{2+} ions are each coordinatively saturated by two Cl ions.

The adsorption energies of CO on PdCl and CuCl are calculated and the corresponding structures are shown in Figure 1a,b. The adsorption energies of CO on PdCl and CuCl are −1.54 and −0.68 eV respectively, which is validated further by in situ DRIFTS spectra (Figure 1c) with two high intensity absorption peaks at 2126 and 1939 cm^{-1} of Cu^{+}–CO and Pd^{+}–CO absorption species, respectively. The above results show that Pd^{+} and Cu^{+} are CO adsorption sites.

Secondly, the O_2 adsorption configurations on PdCl and CuCl calculated by DFT in the absence of H_2O are shown in Figure 2a,b. The adsorption energies of O_2 on PdCl and CuCl are −1.33 and −1.13 eV, respectively. CO absorption configurations on PdCl and CuCl in the presence of O_2 are, however, the same as in Figure 1a,b. DFT calculations show that the adsorp-

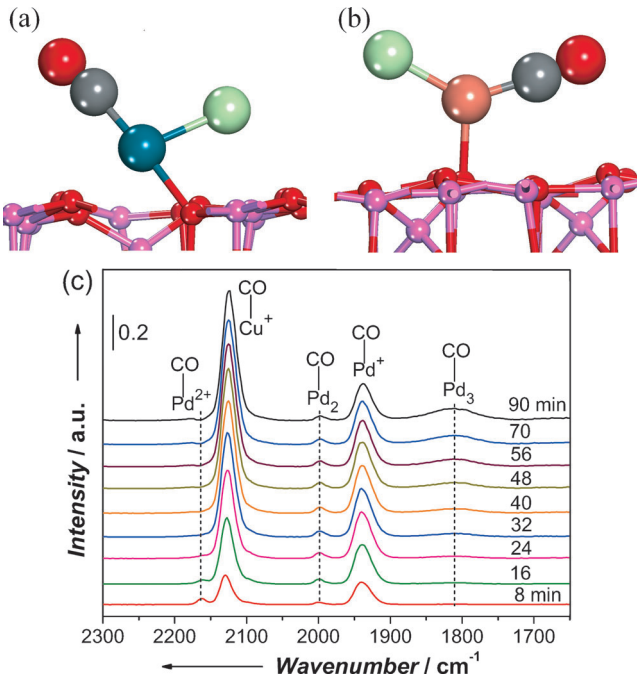

Figure 1. a) Structures of CO adsorbed on the PdCl and b) CuCl species on the γ-Al_2O_3(1 0 0) crystal face (●: C, ●: Pd, ●: Cu, ●: O, ●: Cl, and ●: Al atoms); and c) in situ DRIFTS spectra of CO adsorbed over Pd-Cu-Cl_x/γ-Al_2O_3 at 25 °C.[12]

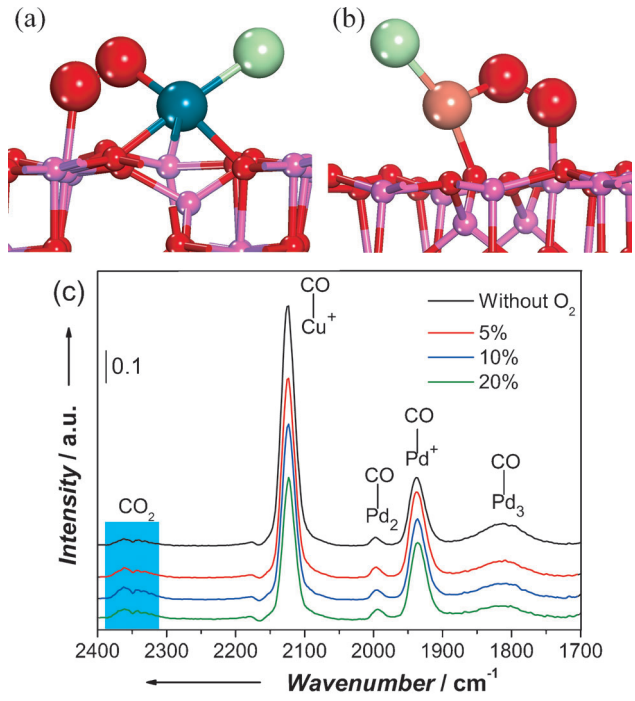

Figure 2. Structures of O_2 adsorbed on a) PdCl and b) CuCl species on the γ-Al_2O_3(1 0 0) crystal face (●: Pd, ●: Cu, ●: O, ●: Cl, and ●: Al atoms); and c) in situ DRIFTS spectra of CO adsorbed over Pd-Cu-Cl_x/γ-Al_2O_3 in different O_2 concentrations at 25 °C.[12]

tion energy of O_2 on PdCl (−1.33 eV) is slightly lower than that of CO on PdCl (−1.54 eV), which indicates that CO is the main absorption species, rather than O_2, on PdCl. This result is validated by in situ DRIFTS spectra (Figure 2c) with a typical absorption peak of Pd^+–CO at 1939 cm^{-1}, which strengthens with an increase in the O_2 concentration.

The adsorption energy of O_2 on CuCl (−1.13 eV) based on DFT calculation is higher than that of CO on CuCl (−0.68 eV), which indicates that O_2 is the main adsorption species, rather than CO, on CuCl. This result is further validated by in situ DRIFTS spectra (Figure 2c) with a typical peak of Cu^+–CO at 2126 cm^{-1}, which weakens clearly with an increase in the O_2 concentration. For single Cu catalysts, the IR absorption peak of Cu^+–CO varies very little with O_2 concentration.[16] The results mentioned above show that CuCl is the main active sites for O_2 adsorption and PdCl is the main active sites of CO adsorption on the Pd-Cu-Cl_x/Al_2O_3 catalyst under an atmosphere of CO and O_2 without H_2O.

Our previous research[4] and that of Koh et al.[9] showed that the CO oxidation at low temperature can be accelerated in presence of water. Thus, the role of H_2O is a key consideration. Adsorption and dissociation of H_2O on the γ-Al_2O_3(1 0 0) facet have been calculated by using DFT, the results of which are shown in Figures S5 and S6. The calculated dissociated energy of H_2O on γ-Al_2O_3(1 0 0) facet is 0.10 eV, which indicates that H_2O can dissociate easily to a proton –H on the O_{3c} site and an –OH group on the Al_{5c} site.

Our calculations indicate that the energy barrier for the –H-promoted $PdCl_2$ dechlorination process is ≈0.14 eV [Eq. (2a)] and, with no –H promotion, $PdCl_2$ dechlorination on Al_2O_3 cannot occur. In this case, PdCl reacts with –OH to form PdClOH [Eq. (2b)], which is easily dechlorinated to PdOH by removal of Cl^- ions with an energy barrier of 0.01 eV [Eq. (2c)]. Relative structural configurations are shown in Figures S7a and S8.

$$PdCl_2 + -H \rightleftharpoons PdCl + HCl \quad (2a)$$

$$PdCl + -OH \rightleftharpoons PdClOH \quad (2b)$$

$$PdClOH + -H \rightleftharpoons PdOH + HCl \quad (2c)$$

For the –H-promoted dechlorination process of $CuCl_2$, the energy barrier is ≈0.10 eV [Eq. (3a)]. Its reaction configurations are shown in Figure S7b. CuCl reacts further with –OH to form CuClOH [Eq. (3b)]. Unlike the adsorption of Pd on the surface O–O bridge site from $PdCl_2$ (Figure S2) to PdOH (Figure 3a), Cu in CuCl–OH can absorb on the O–Al bridge (Figure 3b), hence, there is no empty Al site to accept Cl^- ions. Therefore, CuClOH cannot be further dechlorinated, which is quite different to the case with PdClOH [Eq. (2c)].

$$CuCl_2 + -H \rightleftharpoons CuCl + HCl \quad (3a)$$

$$CuCl + -OH \rightleftharpoons CuClOH \quad (3b)$$

The above results show that PdOH and CuClOH are the main catalytically active species on γ-Al_2O_3 in the water-containing reaction gas (CO and O_2), and their structural configurations are shown in Figure 3a,b. The adsorption of CO and O_2 on PdOH and CuClOH are the key steps for the whole CO oxidation process.

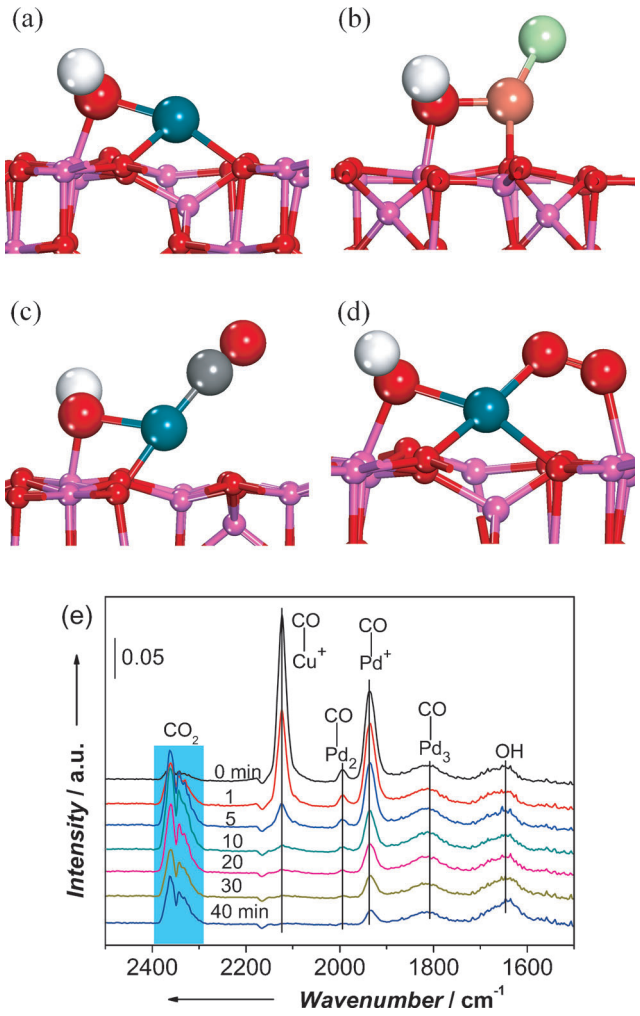

Figure 3. Structural configurations of a) PdClOH, b) CuClOH, c) CO, and d) O_2 adsorbed on PdOH on the γ-Al_2O_3(1 0 0) crystal face (●: H, ●: C, ●: Pd, ●: Cu, ●: O, ●: Cl, and ●: Al atoms); and e) in situ DRIFTS spectra of CO adsorbed over Pd-Cu-Cl_x/γ-Al_2O_3 in the presence of 20% O_2 against the time of H_2O introduction (≈6000 ppm) at 25 °C.[12]

CO can adsorb on PdOH to form a CO–PdOH species with an adsorption energy of −1.74 eV [Figure 3c, Eq. (4)], which is higher than that of O_2 adsorbing on PdOH (−1.29 eV, Figure 3d). This indicates that the species adsorbed on PdOH is mainly CO instead of O_2. This configuration of Pd coordinated with carbonyl and hydroxyl ligands has also been proposed for the carbon-supported Wacker-type catalysts. Park et al.,[17] and Kotareva et al. have proposed analogous reaction intermediates over the $PdCl_2$-$CuCl_2$/γ-Al_2O_3 catalyst.[18]

$$PdOH + CO \rightleftharpoons CO{-}PdOH \quad (4)$$

Further DFT studies show that both CO and O_2 cannot actively adsorb on CuClOH. Based on the above results that O_2 cannot actively adsorb on $PdCl_2$ or $CuCl_2$, we conclude that O_2 adsorbs mainly on CuCl sites and CO mainly on PdOH sites in the presence of water for the Pd-Cu-Cl_x/Al_2O_3 catalyst. Those results are consistent with in situ DRIFTS spectra (Figure 3e): the Cu^+–CO peak at 2126 cm^{-1} disappears quickly after ≈10 min; the Pd^+–CO peak at 1939 cm^{-1} decreases to a steady state, and CuClOH (1645 cm^{-1}) and CO_2 (2300–2400 cm^{-1}) generate quickly.

Based on the results calculated by DFT, we have proposed the catalytic reaction mechanism of Pd-Cu-Cl_x/γ-Al_2O_3 for CO oxidation (Scheme 1). There are two catalytic cycles in the CO oxidation process, the Pd cycle (——) and the Cu cycle (——). The important intermediates or transition states are shown in Figure S9a–o.

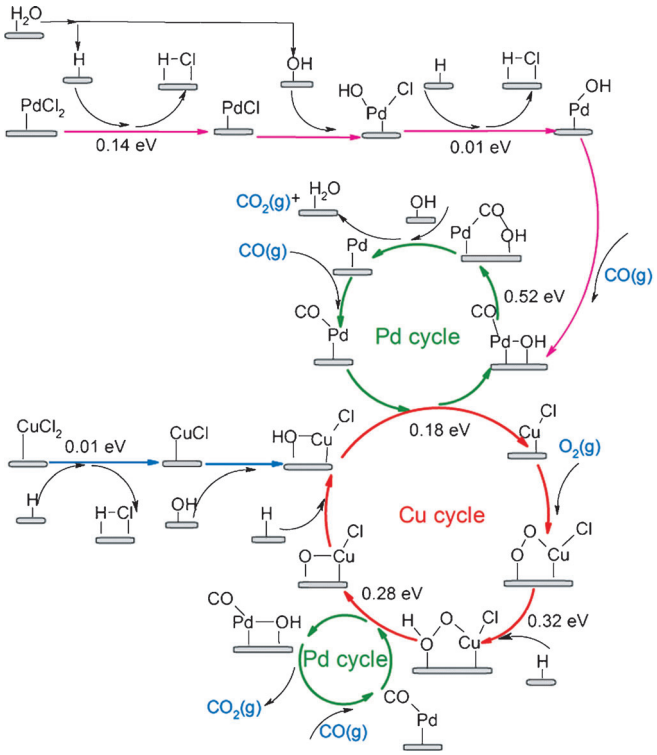

Scheme 1. Proposed catalytic oxidation mechanism of CO over Pd-Cu-Cl_x/Al_2O_3 in the presence of H_2O. The energy marked is an energy barrier.

Pd species catalytic cycle

CO adsorbs on PdOH to form a bidentate CO–Pd–OH species [Figure S9a, Eq. (4)], then the *cis*-PdCOOH intermediate is produced [Figure S9b, Eq. (5a)] with an energy barrier of 0.52 eV. Next, the *cis*-PdCO–OH (Figure S9c) directly dissociates –H to the nearest surface –OH to form adsorbed H_2O (Figure S9d) and Pd–CO_2, then releases CO_2 to the gas phase [Eq. (5b)]. Finally, Pd^0 is produced, which adsorbs CO to form PdCO (Figure S9e,f). PdCO attacks the hydroxyl of CuClOH to form OH–Pd–CO and CuCl species with an energy barrier of 0.18 eV [Figure S9f–h, Eq. (5d)]. Thus, Pd repeats its catalytic cycle to catalyze the CO oxidation.

$$CO{-}PdOH \rightleftharpoons PdCOOH \quad (5a)$$

$$PdCOOH + {-}OH \rightleftharpoons H_2O + Pd^0 + CO_2 \quad (5b)$$

$$Pd^0 + CO \rightleftharpoons PdCO \quad (5c)$$

$$PdCO + CuClOH \rightleftharpoons CuCl + CO{-}PdOH \quad (5d)$$

Notably, the Pd^0 formed as described in Equation (5b) can adsorb CO further to form Pd–CO with an adsorption energy of −1.52 eV, which can be validated by analysis of in situ DRIFTS spectra (Figure 3e), with the absorption peak at 1800 cm^{-1} corresponding to the $-COPd_3$ species.

Cu species catalytic cycle

CuOHCl is attacked by Pd–CO to form CuCl and CO–PdOH [Eq. (5d)], then CuCl located at surface O_{3c} adsorbs O_2 with an adsorption energy of −1.13 eV to produce superoxide Cu species with an O=O bond length of 1.33 Å [Eq. (6a), Figure S9i]. This configuration is hydrogenated very easily by surface –H to form CuClO–OH species with an energy barrier of ≈0.32 eV [Figure S9j–l, Eq. (6b)]. If CuClOOH is attacked by the next PdCO, the O–OH bond is cleaved easily to form CuClO and COPdOH with an energy barrier of 0.28 eV [Figure S9m–o, Eq. (6c)]. CuClO is quite unstable and is hydrogenated by surface –H to form CuClOH [Figure S9p, Eq. (6d)].

$$CuCl + O_2 \rightleftharpoons CuClO_2 \quad (6a)$$

$$CuClO_2 + -H \rightleftharpoons CuClO{-}OH \quad (6b)$$

$$PdCO + CuClO{-}OH \rightleftharpoons CuClO + PdOH \quad (6c)$$

$$CuClO + H \rightleftharpoons CuClOH \quad (6d)$$

In summary, in the catalytic oxidation mechanism of CO: 1) Pd species are mainly the active sites for CO and Cu species the active sites for O_2. 2) A moderate amount of H_2O on the γ-Al_2O_3 surface can promote low-temperature CO oxidation but the presence of excess H_2O would cause formation of a poisonous species, because H_2O is easily dissociated to absorbed –H and –OH species, these can occupy the surface active sites of Pd and Cu. This result has been verified by our previous experimental results.[3,4,12] 3) The energy barrier of the rate-determining step, the transformation of CO–Pd–OH to Pd–COOH, is 0.52 eV. This energy barrier indicates that CO oxidation occurs very easily over Pd-Cu-Cl_x/γ-Al_2O_3. CO_2 formation has been detected by using in situ DRIFTS, for example, the CO_2 absorption peak at 2350 cm^{-1} increases throughout the reaction.

Experimental Section

The 1.7 wt% Pd-3.3 wt% Cu-Cl_x/Al_2O_3 catalyst was prepared by an NH_3 coordination–impregnation method with isopropanol solvent.[3,12] Weighed $PdCl_2$ and $CuCl_2{\cdot}2H_2O$ solid was dissolved in 25% ammonia aqueous solution (2 mL) under ultrasonic shaking at RT and the resulting solution diluted to 8 mL with isopropanol. Then Al_2O_3 (1 g) was impregnated into the solution. After aging for 24 h, the catalyst was dried at RT and calcined at 300 °C for 4 h.

DRIFTS of CO adsorbed on the catalyst was performed on a Nicolet Nexus 670 spectrometer equipped with a mercury cadmium telluride detector. The sample cell was fitted with ZnSe windows and the heating chamber could be heated up to 600 °C.[12] The DRIFTS spectra obtained were saved in Kubelka–Munk a unit with a resolution of 4 cm^{-1} and 64 scans. The catalyst was pretreated in a He flow at 300 °C for 1 h, then cooled to 25 °C, and the background spectrum in a He flow recorded. Then, 1) after the gas mixture of 0.15% CO + O_2 [O_2: 0, 5, 10, and 20% (v/v)] + balanced He had flowed through the sample cell for 30 min at 50 mL min^{-1}, the spectra were recorded at 25 °C; 2) ≈6000 ppm H_2O was added in the gas mixture in step 1 and the spectra were recorded; 3) CO was removed from the gas mixture in step 2 and the spectra were recorded.

DFT calculations were performed within the generalized gradient approximation by using the VASP.[15,19] The project-augmented wave method was used to represent the core–valence interaction.[20] The valence electronic states were expanded in plane-wave basis sets with an energy cut-off at 450 eV. The crystallographic data of γ-Al_2O_3 bulk structure used in this work were taken from the model by Digne et al;[21] optimized lattice parameters of γ-Al_2O_3: $a=5.57$, $b=8.39$, $c=8.05$ Å and $\beta=90.59°$, which was consistent with Digne's results.[21] There were mainly (1 1 0) and (1 0 0) crystal faces in γ-Al_2O_3.[21] However, we had not found the oxidation reaction path of CO on the (1 1 0) crystal faces of γ-Al_2O_3.[13] Therefore, the (1 0 0) crystal face was selected as the calculation model for the γ-Al_2O_3 support. A $p(1\times2)$ surface cell with an area of 11.17×8.41 $Å^2$ corresponding to a 1×1×1 *k*-point mesh was used to fully take the relaxation effects into account. The γ-Al_2O_3(1 0 0)-(1×2) unit cell is shown in Figure S1.

All calculations were performed on a 6-layer slab model containing 24 Al_2O_3 units with a vacuum region of thickness ≈16 Å to prevent interaction between the surface adsorbates on the outer layers and the adjacent slab. We allowed the top two atomic layers of the slab and their adsorbates to relax, whereas the other atomic layers were held fixed at the bulk positions. The transition states were searched for by using a constrained optimization scheme[22] and verified if 1) all forces on atoms vanished and 2) the total energy was a maximum along the reaction coordination but a minimum with respect to the rest of the freedom degrees. The force threshold for the optimization and transition state search was 0.05 eV $Å^{-1}$. In this work, the adsorption (or binding) energy (ΔE_{ad}) of catalyst species (CS; e.g., $PdCl_2$, PdCl, $CuCl_2$, CuCl, and H_2O) on the surface of clean γ-Al_2O_3 were calculated by using Equation (7):

$$\Delta E_{ad} = E_{CS/\gamma-Al_2O_3} - (E_{CS} + E_{\gamma-Al_2O_3}) \quad (7)$$

in which $E_{CS/\gamma-Al_2O_3}$ is the total energy of CS interacting with the clean γ-Al_2O_3 surface, $E_{\gamma-Al_2O_3}$ the total energy of clean γ-Al_2O_3(1 0 0) surface, and E_{CS} the total energy of the catalyst species in vacuum. The total energies of $PdCl_2$, PdCl, $CuCl_2$, CuCl, H_2O, CO, and O_2 were evaluated in a (20×20×20 $Å^3$) supercell by using spin-polarized calculations with the help of the VASP.

The negative value of ΔE_{ad} evidenced an energy gain during adsorption. The adsorption energies of molecules (e.g., CO and O_2) on CS/Al_2O_3 was calculated by using Equation (8):

$$E_{ad} = E^{total}_{mol/CS/\gamma-Al_2O_3} - (E^{total}_{CS/\gamma-Al_2O_3} + E^{free}_{mol}) \quad (8)$$

in which $E^{total}_{mol/CS/\gamma-Al_2O_3}$ represents the total energy of adsorbed molecules (mol) on the CS/Al_2O_3 surface and E^{free}_{mol} the total energy of molecules in the gas-phase. The negative value of E_{ad} evidenced an energy gain during adsorption.

Acknowledgements

This project was supported financially by the National Basic Research Program (2010CB732300, 2013CB933201), the National Natural Science Foundation of China (21273150, 21203119), the Shanghai Natural Science Foundation (12ZR-1430800), and the ShuGuang Project (10GG23), Innovation Program (12YZ161) and Leading Academic Discipline Project (J51503) of Shanghai Municipal Education Commission.

Keywords: copper · density functional calculations · oxidation · palladium · reaction mechanisms

[1] X. W. Xie, Y. Li, Z. Q. Liu, M. Haruta, W. J. Shen, *Nature* **2009**, *458*, 746.
[2] W. S. Lee, B. Z. Wan, C. N. Kuo, W. C. Lee, S. Cheng, *Catal. Commun.* **2007**, *8*, 1604.
[3] Y. X. Shen, G. Z. Lu, Y. Guo, Y. Q. Wang, *Chem. Commun.* **2010**, *46*, 8433.
[4] Y. X. Shen, Y. Guo, L. Wang, Y. Q. Wang, X. Q. Qing, *Catal. Sci. Technol.* **2011**, *1*, 1202.
[5] K. D. Kim, I. S. Nama, J. S. Chung, J. S. Lee, Y. S. Yang, *Appl. Catal. B* **1994**, *5*, 103.
[6] W. G. Lloyd, D. R. Rowe, *Environ. Sci. Technol.* **1971**, *5*, 1133.
[7] K. I. Choi, M. A. Vannice, *J. Catal.* **1991**, *127*, 489.
[8] J. S. Lee, S. H. Choi, K. D. Kim, M. Nomura, *Appl. Catal. B* **1996**, *7*, 199.
[9] D. J. Koh, J. H. Song, S. W. Ham, J. S. Lee, Y. G. Kim, *Korean J. Chem. Eng.* **1997**, *14*, 486.
[10] E. D. Park, J. S. Lee, *J. Catal.* **1998**, *180*, 123.
[11] E. D. Park, S. H. Choi, J. S. Lee, *J. Phys. Chem. B* **2000**, *104*, 5586.
[12] Y. X. Shen, G. Z. Lu, Y. Guo, Y. Q. Wang, Y. L. Guo, X. Q. Qong, *Catal. Today* **2011**, *175*, 558.
[13] C. Shang, Z. P. Liu, *J. Phys. Chem. C* **2010**, *114*, 16989.
[14] H. F. Wang, R. Kavanagh, Y. L. Guo, Y. Guo, G. Z. Lu, P. Hu, *Angew. Chem.* **2012**, *124*, 6761; *Angew. Chem. Int. Ed.* **2012**, *51*, 6657.
[15] G. Kresse, J. Hafner, *Phys. Rev. B* **1994**, *49*, 14251.
[16] K. I. Choi, M. A. Vannice, *J. Catal.* **1991**, *127*, 465.
[17] E. D. Park, K. H. Lee, J. S. Lee, *Catal. Today* **2000**, *63*, 147.
[18] I. A. Kotareva, I. V. Oshanina, K. Yu. Odintsov, L. G. Bruk, O. N. Temkin, *Kinet. Catal.* **2008**, *49*, 18.
[19] G. Kresse, J. Furthmüller, *Comput. Mater. Sci.* **1996**, *6*, 15.
[20] G. Kresse, D. Joubert, *Phys. Rev. B* **1999**, *59*, 1758.
[21] M. Digne, P. Sautet, H. Toulhoat, *J. Catal.* **2004**, *226*, 54.
[22] A. Alavi, P. Hu, T. Deutsch, P. L. Silvestrelli, J. Hutter, *Phys. Rev. Lett.* **1998**, *80*, 3650.

Received: May 7, 2013
Published online on July 24, 2013